



CHORUS

This is the accepted manuscript made available via CHORUS. The article has been published as:

Coexistence of magnetic fluctuations and superconductivity in $\text{SmFe}_{0.95}\text{Co}_{0.05}\text{AsO}$ seen in ^{57}Fe Mössbauer spectroscopy

G. Long, M. DeMarco, M. Chudyk, J. Steiner, D. Coffey, H. Zeng, Y. K. Li, G. H. Cao, and Z. A. Xu

Phys. Rev. B **84**, 064423 — Published 23 August 2011

DOI: [10.1103/PhysRevB.84.064423](https://doi.org/10.1103/PhysRevB.84.064423)

Coexistence of magnetic fluctuations and superconductivity in $\text{SmFe}_{0.95}\text{Co}_{0.05}\text{AsO}$ seen in ^{57}Fe Mössbauer spectroscopy

G. Long,¹ M. De Marco,^{1,2} M. Chudyk,² J. Steiner,² D. Coffey,² H. Zeng,¹ Y.K. Li,³ G. H. Cao,³ and Z. A. Xu³

¹*Dept. of Physics, State University of New York, NY 14260*

²*Dept. of Physics, Buffalo State College, NY 14222*

³*Dept. of Physics, Zhejiang University, Hangzhou 310027, China*

The Mössbauer spectra (MS) of powder samples of $\text{SmFe}_{1-x}\text{Co}_x\text{AsO}$ ($x=0.0, 0.05, \text{ and } 0.1$) were measured in applied fields up to 9 T and at temperatures up to 298 K. SmFeAsO is magnetically ordered with $T_N=137$ K and has a hyperfine magnetic field of (4.98 ± 0.18) T at 4.2 K. In applied magnetic fields the MS is consistent with a distribution of hyperfine magnetic fields of width $H_{\text{applied}} + H_{\text{hyperfine}}$. This arises because the angles between the direction of the ordered field in the crystallites making up the sample are randomly distributed about the direction of the applied field. The MS of the superconductors $\text{SmFe}_{0.95}\text{Co}_{0.05}\text{AsO}$ ($T_C \simeq 5$ K) and $\text{SmFe}_{0.9}\text{Co}_{0.1}\text{AsO}$ ($T_C \simeq 17$ K) are well-described by a single peak from room temperature to 4.2 K indicating the absence of static magnetic order. However the half width at half maximum, Γ , of the peak in $\text{SmFe}_{0.95}\text{Co}_{0.05}\text{AsO}$ increases with decreasing temperature from its high temperature value, 0.13 mm/sec at 25 K, to 0.25 mm/sec at 10 K. No such temperature dependence is seen in $\text{SmFe}_{0.9}\text{Co}_{0.1}\text{AsO}$. We analyze this temperature dependence in terms a fluctuating hyperfine magnetic field model whose frequency at 4.2 K is found to be ~ 5 -10 MHz, giving direct evidence of coexisting magnetic fluctuations and superconductivity at the interface in the phase diagram between the regions with magnetic and superconducting order. In a 5 T applied field $\text{SmFe}_{0.95}\text{Co}_{0.05}\text{AsO}$ is no longer superconducting, however the temperature dependent fluctuating magnetic field is still present and largely unchanged. The absence of fluctuations in superconducting $\text{SmFe}_{0.9}\text{Co}_{0.1}\text{AsO}$ and their presence in superconducting $\text{SmFe}_{0.95}\text{Co}_{0.05}\text{AsO}$ in zero applied field and in non-superconducting $\text{SmFe}_{0.95}\text{Co}_{0.05}\text{AsO}$ at 5T suggests that magnetic order is in competition with superconductivity in $\text{SmFe}_{1-x}\text{Co}_x\text{AsO}$.

PACS numbers: 76.80.+y, 74.25.Dw, 74.70.Xa

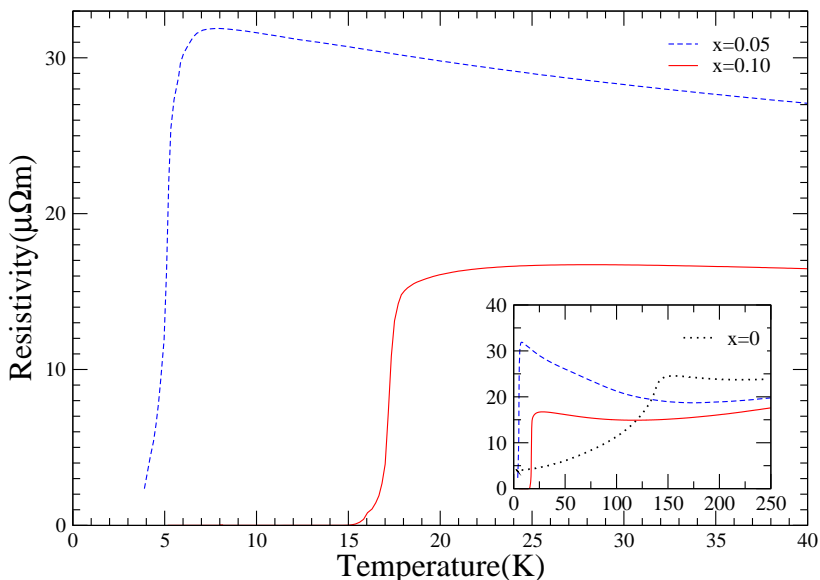


FIG. 1. (Color Online) Resistivity as a function of temperature of the three samples used in this investigation. T_C^{mid} , defined as the midpoint in the resistive transition, is $\simeq 5.1\text{K}$ for $x=0.05$ and 17.2K for $x=0.1$ from Ref.⁴. The inset shows the resistivity for $x=0$, $x=0.05$ and $x=0.1$ samples up to 250K.

I. INTRODUCTION

The discovery of superconductivity in Fe-based layered materials, whose T_C 's can be as high as 55K, has provided a new laboratory for the investigation of high temperature superconductivity in addition to the cuprates. Although there are similarities between the two classes of superconductors, there are also significant differences. Both classes arise from doping antiferromagnetically ordered parent compounds whose magnetic order is suppressed with sufficient doping as superconductivity develops. Superconductivity in turn is destroyed by further doping. The surprising feature of the Fe-based superconductors is that their important component, Fe-As layers, should contain a magnetic element, Fe, which does not act as a pair-breaker in these materials. The Fe-based superconductors can be grouped into different classes. These are, RFeAsO (R=rare earth element) having one Fe-As layer between oxide layers, AFe₂As₂ (A=Sr, Ca, Ba, Eu and K) containing two layers, LiFeAs and Fe_{1+y}As. These are referred to as 1111, 122, 111 and 11 materials, respectively. F doping or O deficiency in the 1111 class has led to a range of superconductors with T_C 's in the 50 K range. The materials of interest here are superconductors which arise from doping Co into the Fe-As layers in the 1111 class. This introduces additional itinerant electrons and disorder. More detailed discussions of the experimental work on these compounds is available in reviews emphasizing magnetic¹ and superconducting properties².

Superconductivity in the 1111 iron pnictides induced by Co doping was first observed in LaFe_{1-x}Co_xAsO^{3,4} and subsequently in SmFe_{1-x}Co_xAsO⁴⁻⁶. Wang et al.⁴ determined the main features of the SmFe_{1-x}Co_xAsO temperature-doping phase diagram using electrical resistivity, susceptibility, thermopower, and x-ray structure analysis. The samples used in this study were among those synthesized and used in the study by Wang et al.⁴. SmFeAsO has a transition from tetragonal to orthorhombic structure at 155 K and to an antiferromagnetic state at 137 K. The size of the magnetic hyperfine magnetic fields at the ⁵⁷Fe site are ~ 5 T at 4.2 K in both LaFeAsO³ and SmFeAsO (result in this paper). As x increases both LaFe_{1-x}Co_xAsO and SmFe_{1-x}Co_xAsO cease to order magnetically and they become superconducting. The superconducting transition temperature, determined by the midpoint of the resistive transition measured by the standard four-terminal method, is $\simeq 5.1\text{K}$ for $x = 0.05$ and $\simeq 17.2\text{K}$ for $x = 0.1$, see Fig. 1 and reference⁴. Beyond $x = 0.1$ T_C decreases and there is no superconductivity beyond $x \simeq 0.20$ ⁴. This doping region for superconductivity is slightly larger than that found in LaFe_{1-x}Co_xAsO, $.25 \leq x \leq .15$ ^{3,4}. T_C for these materials has also been determined from magnetic susceptibility measurements and found to be consistent with values from resistivity. At the Co rich end of the RCoAsO (R=Nd,La,Sm) there is a series of magnetic ground states as the temperature decreases⁷⁻¹⁰.

One of the questions of interest in these materials is the connection between magnetism and superconductivity. The similarity of the phase diagram with that of the cuprates has led to models for a magnetic mechanism for superconductivity in the Fe-based superconductors. Evidence has been found for the coexistence of antiferromagnetic and superconducting phases in Ba(Fe_{0.953}Co_{0.047})₂As₂¹¹⁻¹⁵ and for the coexistence of magnetic fluctuations and superconductivity in SmFeAsO_{1-x}F_x^{16,17,21}. This coexistence is complicated by the fact that both ordered phases are determined by the same population of Fe 3d electrons which predominantly populate the states at the Fermi energy²². Here we show that magnetic fluctuations coexist with supercon-

ductivity in $\text{SmFe}_{0.95}\text{Co}_{0.05}\text{AsO}$ and are present also when $\text{SmFe}_{0.95}\text{Co}_{0.05}\text{AsO}$ is driven normal by an applied magnetic field, but are absent in $\text{SmFe}_{0.9}\text{Co}_{0.1}\text{AsO}$.

II. EXPERIMENTAL TECHNIQUES

The synthesis and characterization of the samples used in this study have been discussed previously by Wang et al.⁴. They found the samples to have powder x-ray diffraction spectra well characterized by a single tetragonal structure, indicating phase purity. As we point out below the MS of $\text{SmFe}_{0.95}\text{Co}_{0.05}\text{AsO}$ and $\text{SmFe}_{0.9}\text{Co}_{0.1}\text{AsO}$ are well described by single Fe site fits with and without applied fields. This is further support that the samples have negligible amounts of any impurity phase, if any.

The MS were measured on samples of SmFeAsO ($50\text{mg}/\text{cm}^2$), $\text{SmFe}_{0.95}\text{Co}_{0.05}\text{AsO}$ ($61\text{mg}/\text{cm}^2$) and $\text{SmFe}_{0.9}\text{Co}_{0.1}\text{AsO}$ ($50\text{mg}/\text{cm}^2$) which are equivalent to $0.2\text{ mg}/\text{cm}^2$ or less of ^{57}Fe . The sample holders were made of a carbon based material, delrin. Measurements were made in two different Janis cryostats using $^{57}\text{Co}(\text{Rh})$ sources. A 50 mCi source was used for the magnetic cryostat (solenoid) and a 5 mCi source was used in the smaller zero magnetic cryostat. The velocity calibration was performed by using the six-line spectrum measured using the above sources and metallic α iron foil as an absorber. Both cryostats used transmission geometry with the source and absorber inside the sample chamber. The operation of the Mössbauer probe for the zero magnetic field cryostat has been described previously in other studies²⁴.

The Mössbauer probe which fits into the larger cryostat was constructed using G10 tube material. The Mössbauer transducer (at the top of the cryostat) was connected to two concentric G10 tubes of different diameters connected together near the source by a centering two dimensional spring. The inner tube was fixed to the source and outer tube held to the sample to be studied. The sample was positioned below the source in the center of the solenoid magnet. The magnet is capable of producing up to 9T at the sample. The source is in a nearly zero magnetic field produced by magnetic cancelling coil at the top of the superconducting solenoid magnet. The detector was a Xenon or Krypton gas filled (2 Atmospheres) proportional counter. This detector, 12 inches from the source, was positioned below the mylar window of the cryostat and it was in a maximum magnetic field of 0.015T, minimized by using a cancelling coil at the bottom of the magnet. The temperature was maintained by passing helium gas through a needle valve from the liquid helium reservoir into the sample chamber from the bottom of the cryostat, which then drifts upward to the sample. Two Cernox diode thermometers, one at the sample holder and one at the bottom of the chamber were used for temperature measurements and were controlled by Lakeshore devices. Sample heating was accomplished by heating the gas as it passed through the needle valve at the bottom of the chamber. In the experiments the applied magnetic field is parallel to the direction of propagation of the incident γ -ray.

III. RESULTS

We investigated three materials. In the case of $\text{SmFe}_{0.95}\text{Co}_{0.05}\text{AsO}$ and $\text{SmFe}_{0.9}\text{Co}_{0.1}\text{AsO}$ the MS are single peaks at 4.2 K in the absence of an applied magnetic field showing no evidence of magnetic impurity phases²⁵. A small contribution to the measured MS from Fe impurities in the Al stripes of the Mylar windows was subtracted from the spectra.

The isomer shifts (IS) relative to metallic α Fe-foil is the same for SmFeAsO , $\text{SmFe}_{0.95}\text{Co}_{0.05}\text{AsO}$ and $\text{SmFe}_{0.9}\text{Co}_{0.1}\text{AsO}$, (0.42 ± 0.02) mm/sec, showing that the charge state of the Fe site is not affected by Co doping for $0 \leq x \leq 0.1$ in spite of the evolution from antiferromagnetism to superconductivity.

A. SmFeAsO

The MS for SmFeAsO at 4.2 K in the absence of an applied magnetic field and in a 5T applied field are shown in Fig. 2. Consistent with the $T_N=137$ K for the sample, the MS shows a hyperfine magnetic field at the Fe nucleus. The full line is the calculated spectrum with $H_{\text{hyperfine}}=(4.98 \pm 0.18)$ T and a quadrupole tensor whose principal axis is at an angle to the direction of the hyperfine magnetic field. In the absence of a hyperfine magnetic field, the quadrupole tensor, \mathbf{Q} , would lead to a splitting of $\Delta E_Q \simeq 0.1$ mm/sec so that the elements of \mathbf{Q} are modest but are required to reproduce the asymmetry in the spectrum. The other parameters in the fit are the isomer shift (IS) and the half width at half maximum (Γ_0). The value of the parameters in the fit are those which minimise the sum of the squares of the differences between the calculated spectrum and the data. Given the information from neutron scattering regarding the direction of the ordered moments in LaFeAsO ²³, we assume that the hyperfine magnetic field is parallel to the orthorhombic a -axis, in which case the principal axis of \mathbf{Q} lies in the ac -plane.

The MS undergoes significant changes as the strength of the magnetic field increases beyond 1 T. The six-line spectrum in zero field evolves into a broad spectrum which is almost featureless except for two central peaks in a 5T applied field. This change arises because the hyperfine magnetic field at the Fe nuclei in each crystallite results from two contributions: the magnetic order in that crystallite and the external field. Since the relative orientation of the two contributions is random there is a distribution in both the magnitude of the resulting field and in its direction relative to the direction of propagation of the incident γ -ray. This

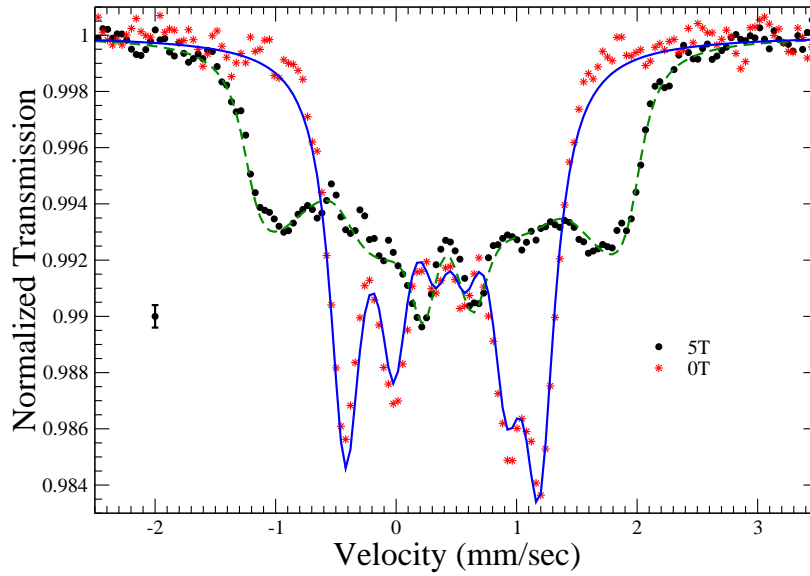


FIG. 2. (Color Online) MS of SmFeAsO at 4.2 K for no applied field and in a 5T applied field. The full line through the zero field data is a single-site fit with a hyperfine magnetic field of (4.98 ± 0.18) T, $IS = (0.42 \pm 0.02)$ mm/sec and $\Gamma_0 = (0.15 \pm 0.015)$ mm/sec. The principal axis of the quadrupole tensor is at an angle to the direction the hyperfine magnetic field. The small quadrupole contribution, $\Delta E_Q \simeq 0.1$ mm/sec, is required to reproduce the asymmetry in the spectrum. The MS of SmFeAsO at 4.2 K in 5 T applied field is broader and lacks the strong lines of the spectrum in the absence of an applied field. The dashed line is MS calculated from an average over a distribution of sites where the hyperfine field has different values and orientations with respect to the direction of the incident γ -ray. The isolated vertical line on the left hand side of the figure indicates the size of the uncertainty in the data points.

happens because the ordered moments in each crystallite cannot lower their energy by flopping into the plane perpendicular to the applied field and canting into the direction of the field due to the strong magnetic anisotropy as evidenced in the local moment fits to measured spin excitation energies¹. The spectrum also depends sensitively on the angle between between the direction of the hyperfine magnetic field at the Fe nucleus and the direction of the incident γ -ray through the usual selection rules. The calculated MS (dashed line) which results from averaging over a uniform distribution of crystallite orientations is compared with the measured MS at 4.2 K in a 5 T applied field in Fig. 2.

B. $\text{SmFe}_{0.95}\text{Co}_{0.05}\text{AsO}$ and $\text{SmFe}_{0.9}\text{Co}_{0.1}\text{AsO}$

In Fig. 3(a) the MS of $\text{SmFe}_{0.95}\text{Co}_{0.05}\text{AsO}$ are plotted for different temperatures in the absence of an applied magnetic field. The MS consist of a single peak indicating that there is no static magnetic order or any indication of impurity phases in the sample. The full width half maximum of the line decreases from 0.50 mm/sec at 4.2 K to 0.26 mm/sec at 25 K. At 78 K the full width half maximum line width is 0.26 mm/sec which is experimentally narrow, indicating the absence of an electric quadrupole contribution to the spectrum. This value determines the value of intrinsic half width half maximum, $\Gamma_0 = 0.13$ mm/sec in our analysis of the spectra. The superconducting transition temperature of $\text{SmFe}_{0.95}\text{Co}_{0.05}\text{AsO}$ was estimated to be ~ 5.1 K from resistivity⁴. A temperature dependent linewidth has also been reported in $\text{LaO}_{.96}\text{F}_{.04}\text{FeAs}$ ²⁶.

In Fig 3(b) the MS is shown for different temperatures in 5 T applied field. The spectra consist of four peaks consistent with a uniform applied field, parallel to direction of the incident γ -ray. The relative positions of the peaks are consistent with pure Zeeman Hamiltonians for the ground and excited states of the ^{57}Fe nucleus and show no evidence of an electric quadrupole contribution, which is consistent with the high temperature spectrum of the sample in the absence of an applied field.

We analyze this temperature dependence of the MS using the fluctuating hyperfine magnetic field model developed by Blume and coworkers^{27,28}. Since our data indicates that there is no static hyperfine magnetic field or significant quadrupole contribution to the spectrum in $\text{SmFe}_{0.95}\text{Co}_{0.05}\text{AsO}$, we attribute the temperature dependent linewidth to be due to a fluctuating hyperfine magnetic field at the Fe nucleus. This hyperfine magnetic field arises from the thermally disordered magnetism in the FeAs layers. The Hamiltonian describing the system in a given nuclear state(ground, $n = gr$, or excited, $n = ex$) is

$$H = -g_n \mu_n \sum_{j=1, N} H_{fj}^j I_j f_j(t) - g_n \mu_n I_z H_{applied} \quad (1)$$

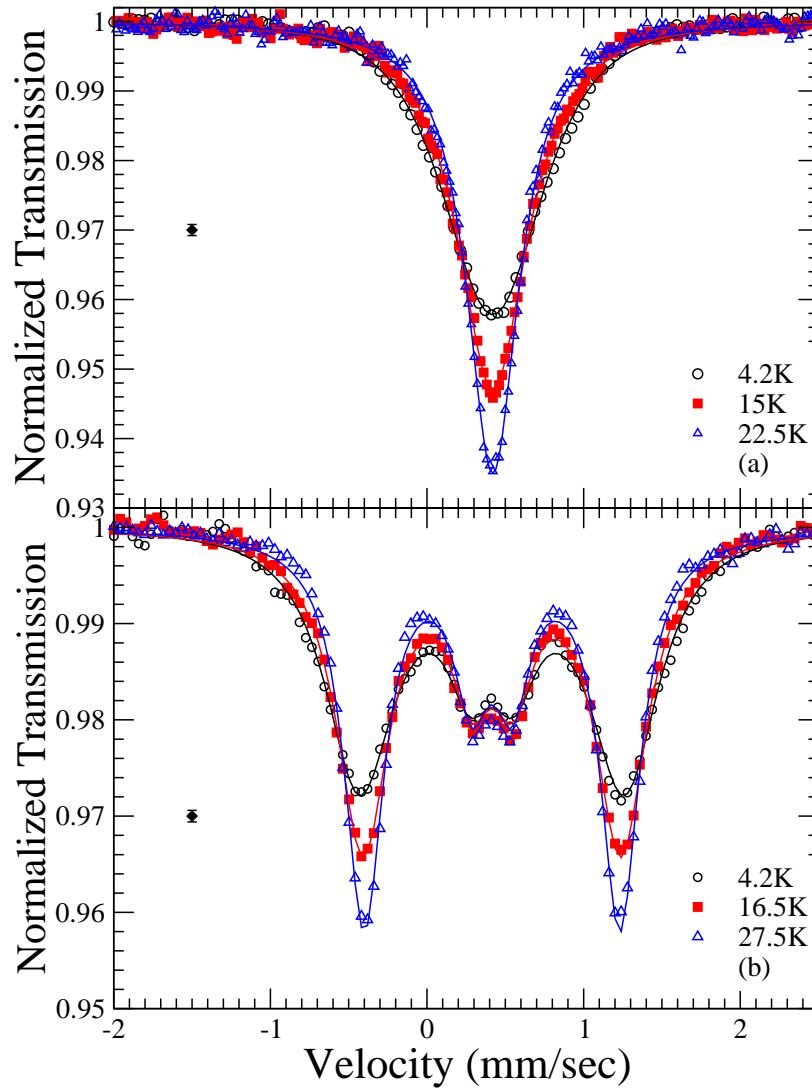


FIG. 3. (Color Online)(a) MS of $\text{SmFe}_{0.95}\text{Co}_{0.05}\text{AsO}$ is a single line spectrum in the absence of an applied magnetic field. The full width half maximum of the line decreases from 0.50 mm/sec at 4.2 K to 0.26 mm/sec at 78 K. (b) MS of $\text{SmFe}_{0.95}\text{Co}_{0.05}\text{AsO}$ in a 5T applied field is a four line spectrum. In both the absence of an applied field and in 5 T applied field, linewidths increase as the temperature decreases. The isolated symbol in each part of the figure indicates the size of the uncertainty in the data.

where g_n is the gyromagnetic factor of the nuclear state, μ_n is the nuclear Bohr magneton, the sum runs over the N directions among which the hyperfine magnetic field fluctuates, I_j is the component of the nuclear spin along direction j , and $f_j(t)$ is a random function of time with values corresponding to different directions. In the absence of a quadrupole contribution which might provide a reference set of axes for these directions, we consider fluctuations among three mutually perpendicular directions, $\pm\hat{x}$, $\pm\hat{y}$ and $\pm\hat{z}$. There is no correlation between the directions of the fluctuating hyperfine magnetic field and this is incorporated in the calculation through a random phase treatment in averaging over the possible changes in directions, j , and a trace over the product space of the nuclear states $|I_{gr}m\rangle > |I_{ex}m'\rangle$ ²⁸.

The parameters in this model which describe the fluctuating field are the amplitude, H_{fl} , and the rate at which the direction of the field switches, $\frac{1}{\tau}$. In the absence of an applied field we assume that the fluctuating hyperfine magnetic field, H_{fl} , is isotropic; while in the presence of an applied field of 5 T, we allow different values of the fluctuating field, parallel ($H_{fl||}$), and perpendicular ($H_{fl\perp}$), to the applied field.

The amplitude of the randomly fluctuating hyperfine magnetic field is assumed to be the same with or within an applied magnetic field and to be independent of temperature. Its value is determined by fitting to the spectrum at 4.2K in a 5 T applied magnetic field. The parameters in the fit are $H_{fl||}$, $H_{fl\perp}$, $\frac{1}{\tau}$ and the IS. The intrinsic half-width half-maximum, Γ_0 , in

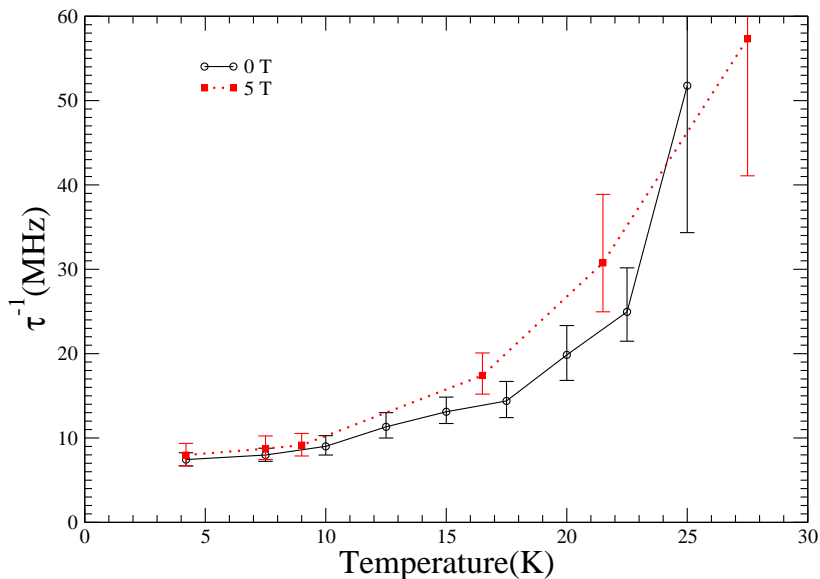


FIG. 4. (Color Online) Relaxation rate of magnetic fluctuations, τ^{-1} , in $\text{SmFe}_{0.95}\text{Co}_{0.05}\text{AsO}$ as a function of temperature. The lines are intended as guides to the eye only.

the absence of the fluctuating hyperfine magnetic field in the high temperature spectra, is as discussed above and found to be $\Gamma_0=0.13$ mm/s. It is found that $H_{fl\parallel}$ and $H_{fl\perp}$ are essentially $\simeq 3.08T$. This value for the amplitude of the fluctuating hyperfine magnetic field is used at other temperatures both in the absence of an applied field and in presence of a 5T applied field. The resulting fits using the hamiltonian in equation (1) are full lines in Fig. 2. The temperature dependence of the linewidths arises from the temperature dependence of $\frac{1}{\tau}$ which is shown in Fig 4. As the temperature increases $\frac{1}{\tau}$ increases, so that the effect of the fluctuating field on the spectra decreases. The error bars are determined by doubling the sum of the square of the difference between the data and calculated spectrum found in the best fit to the data. As the effect of the fluctuating field decreases the fits becoming increasingly insensitive to $\frac{1}{\tau}$ and the size of the error bars grow. Beyond $\sim 25K$ the contribution of the fluctuations to the linewidth is almost negligible. Examining the MS of $\text{SmFe}_{0.95}\text{Co}_{0.05}\text{AsO}$ in a 5 T applied field at 27.5 K we see that the spectrum can be well described by a unique Fe site with $\Gamma_0=0.13$ mm/sec and an isomer shift of $(0.42 \pm .02)$ mm/sec, just as in SmFeAsO . $\frac{1}{\tau}$ is seen to be independent of the applied field. This insensitivity to applied magnetic fields is also seen in the spin-lattice relaxation time, T_1 , in ^{75}As NMR data on $\text{LaFeAsO}_{0.7}$ ¹⁹ and $\text{LaFeAsO}_{0.89}\text{F}_{0.11}$ ²⁰ up to ~ 12 T.

The MS of $\text{SmFe}_{0.9}\text{Co}_{0.1}\text{AsO}$ in zero applied field and in 9 T are shown in Fig 5. The MS at 4.2 K is plotted with the 298 K MS, which has been rescaled to compensate for the temperature dependence of the recoil free fraction. The MS is a single line, showing that there is no static ordered magnetic field, and the width is clearly independent of temperature. The single line MS in the absence of an applied field and the positions of the lines in the MS at 9T points to a negligible electric quadrupole contribution to the spectrum. Just as in the case of the $\text{SmFe}_{0.95}\text{Co}_{0.05}\text{AsO}$ spectrum, the single site fits to the zero field and 9T spectra demonstrate the absence of impurity phases in the $\text{SmFe}_{0.9}\text{Co}_{0.1}\text{AsO}$ sample.

The MS at 4.2 K of $\text{SmFe}_{0.95}\text{Co}_{0.05}\text{AsO}$ in 5 T and $\text{SmFe}_{0.9}\text{Co}_{0.1}\text{AsO}$ in a 9 T field are similar to that of superconducting $\text{LaFeAsO}_{0.89}\text{F}_{0.11}$ in a 5 T field.³⁶ These spectra are indicative of a sample in a uniform magnetic field applied parallel to the direction of propagation of the incident γ -ray. The absence of any field inhomogeneity due to a vortex lattice in the MS shows that these samples have been driven normal by the applied magnetic fields. The measured onset of diamagnetism falls rapidly with increasing applied field and is completely absent above 1 T in $\text{SmFe}_{0.9}\text{Co}_{0.1}\text{AsO}$ (not shown). This is consistent with the absence of diamagnetism measured for $\text{LaFe}_{1-x}\text{Co}_x\text{AsO}$ at 1 T³.

IV. DISCUSSION

We report here the temperature and external magnetic field dependence of Mössbauer spectra of $\text{SmFe}_{1-x}\text{Co}_x\text{AsO}$. We find evidence of magnetic fluctuations at low temperatures for $x=0.05$. These fluctuations are present in $\text{SmFe}_{0.95}\text{Co}_{0.05}\text{AsO}$, with no evidence of static magnetic order, both in the absence of an applied field at 4.2 K, where the material is superconducting, and in 5 T, where it is in the normal phase. There is no significant difference in the temperature dependences of τ^{-1} between the

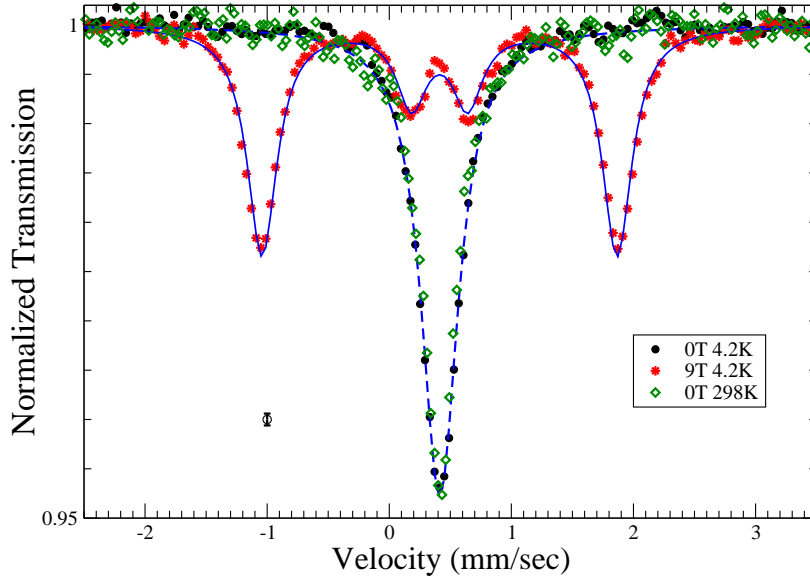


FIG. 5. (Color Online) MS of $\text{SmFe}_{0.9}\text{Co}_{0.1}\text{AsO}$ in the absence of an applied magnetic field at 4.2 K (\bullet) and 298K (\diamond), indicating the absence of any temperature dependence in the linewidth or magnetic impurities in the sample. The full line is a fit with $\text{IS}=(0.41\pm.02)$ mm/sec and $\Gamma_0=(0.18\pm.01)$ mm/sec. MS of $\text{SmFe}_{0.9}\text{Co}_{0.1}\text{AsO}$ in a 9 T applied magnetic field at 4.2K($*$). The full line is calculated MS for a 9 T applied field. The IS is $(0.41\pm.02)$ mm/sec and $\Gamma_0=(0.15\pm.02)$ mm/sec. The uncertainty in the data points is the size of the symbols used to represent them, as shown by the symbol at the lower left of the figure.

zero applied field case (superconducting) and when there is a 5 T applied field (non-superconducting).

These fluctuations are probably due to Fe moments. This is because the fluctuations are seen at $x = 0.05$ and not at $x = 0.1$, which is further from the region of the phase diagram where magnetic order is found. This enhancement of fluctuation effects has also been identified in ^{75}As NMR spin-lattice relaxation time in $\text{Ba}(\text{Fe}_{1-x}\text{Co}_x)\text{As}_2$ ¹⁸, $\text{LaFeAsO}_{0.7}$ ¹⁹ and $\text{LaFeAs}(\text{O}_{0.89}\text{F}_{0.11})$ ²⁰. In these materials there is an enhancement of $(T_1T)^{-1}$ as $T \rightarrow T_N$, (T_N is the ordering temperature of the Fe moments). As doping levels increase and the materials no longer order magnetically, this enhancement goes away. The interpretation of this data has been that this enhancement is due to the critical slowing down of spin fluctuations and their absence for larger doping levels is consistent with our results for $x = 0.05$ and $x = 0.1$, reported here for $\text{SmFe}_{1-x}\text{Co}_x\text{AsO}$.

There are also moments on the Sm sites, which are seen to order in $\text{SmO}_{1-x}\text{F}_x\text{FeAs}$ at 4.6 K ($x = 0$) and at 3.7 K ($x = 0.15$) in specific heat.²⁹ Sharp peaks are seen in the data at both doping values. It is difficult to see how the fluctuations seen in $\text{SmFe}_{0.95}\text{Co}_{0.05}\text{AsO}$ could be due to the incipient ordering of Sm moments, given the strong dependence on Co-doping of the fluctuation effects. The signature of magnetic fluctuations were also seen in μSR by Drew et al.¹⁶, again in $\text{SmO}_{1-x}\text{F}_x\text{FeAs}$. They found that muon relaxation is much slower at $x = 0.30$ than at $x = 0.18$, closer to the region of Fe ordering and pointed to this as evidence against the fluctuations being associated with the Sm moments.

The frequencies of the fluctuations in $\text{SmFe}_{0.95}\text{Co}_{0.05}\text{AsO}$, $\sim 10 - 20$ MHz where they have a significant contribution to the linewidths, are very much smaller than the frequencies characterizing spin dynamics in these materials³⁰ or the spin resonance mode seen below T_C in $\text{Ba}(\text{Fe}_{1-x}\text{Co}_x)\text{AsO}$ ^{31,32} and so they are most likely associated with the proximity to the ordered magnetic phase. The amplitude of the fluctuations is roughly half the hyperfine magnetic field in magnetically ordered SmFeAsO . This suggests that the effects of Co doping at $x=0.05$ are just enough to prevent static magnetic order at 4.2K and above. Fixing the amplitude of the fluctuations of the hyperfine magnetic field to its value at 4.2K, the fluctuation effects go away due to the increase in the rate at which the hyperfine magnetic field randomly switches direction with temperature. The origin of the hyperfine magnetic field is the random fluctuations in the directions of electronic moments at the Fe sites. The increase in the fluctuation rate with temperature is similar to the behavior found by Moessner and Chalker³⁴ in their investigation of small fluctuations about the ground state configurations in a geometrically frustrated antiferromagnet. They used a classical Heisenberg model on the pyrochlore lattice and found $\tau^{-1} \propto T$. τ^{-1} appears to approach ~ 10 MHz in zero applied and in a 5 T applied field and starts to increase beyond ~ 10 K. We do not have a microscopic model for how these fluctuations found in $\text{SmFe}_{0.95}\text{Co}_{0.05}\text{AsO}$ evolve. A similar analysis has been carried out by Bonville et al.³⁷ on the temperature dependence of the relaxation rate in $\text{Gd}_3\text{Ga}_5\text{O}_{12}$ using the ^{155}Gd Mössbauer effect. However the absence of these fluctuations in $\text{SmFe}_{0.9}\text{Co}_{0.1}\text{AsO}$, where superconductivity is more robust ($T_C \simeq 17\text{K}$), suggests that magnetism and superconductivity are in competition with one another in $\text{SmFe}_{1-x}\text{Co}_x\text{AsO}$ rather than spin fluctuations coexisting with superconductivity and pointing to a possible magnetic

mechanism for superconductivity.

V. ACKNOWLEDGMENTS

This work was supported by USDOE(DE-FG02-03ER46064) and NSF(DMR-0547036) in Buffalo and the Chinese National Science Foundation(Contract No. 10674119 and Contract No, 10634020) in Hangzhou.

-
- ¹ M. D. Lumsden and A. D. Christianson, *J. Phys. Condens. Matter*, **22**, 203203 (2010), arXiv:1004.1969.
- ² D. C. Johnston, arXiv:1005.4392, *Advances in Physics* (2010).
- ³ A. S. Sefat, A. Huq, M. A. McGuire, R. Jin, B. C. Sales, D. Mandrus, L. M. D. Cranswick, P. W. Stephens, and K. H. Stone, *Phys. Rev. B* **78**, 104505 (2008).
- ⁴ C. Wang, Y. K. Li, Z. W. Zhu, S. Jiang, X. Lin, Y. K. Luo, S. Chi, L. J. Li, Z. Ren, M. He, H. Chen, Y. T. Wang, Q. Tao, G. H. Cao, and Z. A. Xu, *Phys. Rev. B* **79**, 054521 (2009). See also arXiv.0807.1304 and arXiv.0808.3254.
- ⁵ Y. Qi, Z. Gao, L. Wang, D. Wang, X. Zhang, and Y. Ma, *Supercond. Sci. Technol.* **21**, 115016 (2008).
- ⁶ V.P.S. Awana, A. Vajpayee, A. Pal, M. Mudgel, R. S. Meena, and H. Kishan, *J. Supercond. Nov. Magn.*, **22**, L623 (2009).
- ⁷ M. A. McGuire, D. J. Gout, V. O. Garlea, A. S. Sefat, B. C. Sales, and D. Mandrus, *Phys. Rev. B* **81**, 104405 (2010).
- ⁸ H. Yanagi, R. Kawamura, T. Kamiya, Y. Kamihara, M. Hirano, T. Nakamura, H. Osawa, and H. Hosono, *Phys. Rev. B* **77**, 224431 (2008).
- ⁹ W. Tian, W. Ratcliff, M. G. Kim, J.-Q. Yan, P. A. Kienzle, Q. Huang, B. Jensen, K. W. Dennis, R. W. McCallum, T. A. Lograsso, R. J. McQueeney, A. I. Goldman, J. W. Lynn, and A. Kreyssig, *Phys. Rev B* **82**, 60514(R) (2010).
- ¹⁰ V.P.S. Awana, I. Nowik, A. Pal, K. Yamaura, E. Takayama-Muromachi, and I. Felner, *Phys. Rev. B* **81**, 212501 (2010).
- ¹¹ D. K. Pratt, W. Tian, A. Kreyssig, J. L. Zarestky, S. Nandi, N. Ni, S. L. Bud'ko, P. C. Canfield, A. I. Goldman, and R. J. McQueeney, *Phys. Rev. Lett.* **103**, 087001 (2009).
- ¹² A. D. Christianson, M. D. Lumsden, S. E. Nagler, G. J. MacDougall, M. A. McGuire, A. S. Sefat, R. Jin, B. C. Sales, and D. Mandrus, *Phys. Rev. Lett.* **103**, 087002(2009).
- ¹³ Y. Laplace, J. Bobroff, F. Rullier-Albenque, D. Colson, and A. Forget, *Phys. Rev. B* **80**, 140501 (2009).
- ¹⁴ P. Marsik, K. W. Kim, A. Dubroka, M. Rössle, V. K. Malik, L. Schulz, C. N. Wang, Ch. Niedermayer, A. J. Drew, M. Willis, T. Wolf, and C. Bernhard, *Phys. Rev. Lett.* **105**, 057001 (2010).
- ¹⁵ P. Bonville, F. Rullier-Albenque, D. Colson, and A. Forget, *Europhysics Lett.* **89**, 67008 (2010).
- ¹⁶ A. J. Drew, F. L. Pratt, T. Lancaster, S. J. Blundell, P. J. Baker, R. H. Liu, G. Wu, X. H. Chen, I. Watanabe, V. K. Malik, A. Dubroka, K. W. Kim, M. Rössle, and C. Bernhard, *Phys. Rev. Lett.* **101**, 097010 (2008).
- ¹⁷ S. Sanna, R. De Renzi, G. Lamura, C. Ferdeghini, A. Palenzona, M. Putti, M. Tropeano, and T. Shiroka, *Phys. Rev. B* **80**, 052503 (2009).
- ¹⁸ I. F. Ning, K. Ahilan, T. Imai, A. S. Sefat, R. Jin, M. A. McGuire, B. C. Sales and D. Mandrus, *J. Phys. Soc. Jap.*, **78**, 013711 (2009).
- ¹⁹ N.Terasaki, H. Mukuda, M. Yashima, Y. Kitaoka, K. Miyazawa, P. M. Shirage, H. Kito, H. Eisaki, and A. Iyo, *J. Phys. Soc. Jap.*, **78**, 013701 (2009).
- ²⁰ Y.Nakai, S. Kitagawa, K. Ishida, Y. Kamihara, M. Hirano, and H. Hosono, *New Journal of Physics* **11**, 045004 (2009).
- ²¹ S. Takeshita, R. Kadona, M. Hiraishi, M. Miyazaki, A. Koda, Y. Kamihara, and H. Hosono, *J. Phys. Soc. Jpn* **77**, 103703 (2008).
- ²² D. J. Singh and M. H. Du, *Phys. Rev. Lett.* **100**, 237003 (2008).
- ²³ C. de la Cruz, Q. Huang, J. W. Lynn, J. Li, W. Ratcliff, J. L. Zalestky, H. A. Mook, G. F. Chen, J. L. Luo, N. L. Wang and P. Dai, *Nature* **453**, 899 (2008).
- ²⁴ M. DeMarco, G. Cao, J. E. Crow, D. Coffey, S. Toorongian, M. Haka, and J. Fridmann, *Phys. Rev. B* **62**, 14297 (2000).
- ²⁵ I. Nowik and I. Felner, arXiv:0806.4078.
- ²⁶ H. Luetkens, H.-H. Klauss, M. Kraken, F. J. Litterst, T. Dellmann, R. Klingeler, C. Hess, R. Khasanov, A. Amato, C. Baines, M. Kosmala, O. J. Schumann, M. Braden, J. Hamann-Borrero, N. Leps, A. Kondrat, G. Behr, J. Werner and B. Büchner, *Nature Materials* **8**, 305 (2009).
- ²⁷ M. Blume and J. A. Tjon, *Phys. Rev.* **165**, 446 (1968).
- ²⁸ S. Dattagupta, *Phys. Rev. B* **16**, 158 (1977).
- ²⁹ L. Ding, C. He, J. K. Dong, T. Wu, R. H. Liu, X. H. Chen, and S. Y. Li, *Phys. Rev. B* **77**, 180510(R) (2008).
- ³⁰ K. Matan, S. Ibuka, R. Morinaga, Songxur Chi, J. W. Lynn, A. D. Christianson, M. D. Lumsden, and T. J. Sato, *Phys. Rev. B* **82**, 054515 (2010).
- ³¹ M. D. Lumsden, A. D. Christianson, D. Parshall, M. B. Stone, S. E. Nagler, G. J. MacDougall, H. A. Mook, K. Lokshin, T. Egami, D. L. Abernathy, E. A. Goremychkin, R. Osborn, M. A. McGuire, A. S. Sefat, R. Jin, B. C. Sales, and D. Mandrus, *Phys. Rev. Lett.* **102**, 107005 (2009).
- ³² D. K. Pratt, A. Kreyssig, S. Nandi, N. Ni, A. Thaler, M. D. Lumsden, W. Tian, J. L. Zarestky, S. L. Bud'ko, P. C. Canfield, A. I. Goldman, and R. J. McQueeney, *Phys. Rev. B* **81**, 140510(R)(2010).
- ³³ X. F. Wang, T. Wu, G. Wu, H. Chen, Y. L. Xie, J. J. Ying, Y. J. Yan, R. H. Liu, and X. H. Chen, *Phys. rev. Let.* **102**, 117005 (2009).
- ³⁴ R. Moessner and J. T. Chalker, *Phys. Rev. Lett.* **80**, 2929 (1998); *Phys. Rev. B* **58**, 12049 (1998).
- ³⁵ A. Pal, M. Husain, H. Kishan, and V.P.S. Awana, arVix:1007.5121.
- ³⁶ S. Kitao, Y. Kobayashi, S. Higashitaniguchi, M. Saito, Y. Kamihara, . Hirano, T. Mitsui, H. Hosono, and M. Seto, *J. Phys. Soc. Jap* **77**, 103706 (2008).
- ³⁷ P. Bonville, J. A. Hodges, J. P. Sanchez and P. Vulliet, *Phys. Rev. Lett.* **92**, 167202 (2004).